

# Constraints on $L_\mu - L_\tau$ Gauge Interactions from Rare Kaon Decay

Masahiro Ibe,<sup>1,2,\*</sup> Wakutaka Nakano,<sup>1,2,†</sup> and Motoo Suzuki<sup>1,2,‡</sup>

<sup>1</sup>*Kavli IPMU (WPI), UTIAS, The University of Tokyo, Kashiwa, Chiba 277-8583, Japan*

<sup>2</sup>*ICRR, The University of Tokyo, Kashiwa, Chiba 277-8582, Japan*

(Dated: November 28, 2016)

## Abstract

The model with the  $L_\mu - L_\tau$  gauge symmetry is the least constrained model as a resolution to the disagreement of the muon anomalous magnetic moment between the theoretical prediction and the experimental result. In this paper, we discuss how well the  $L_\mu - L_\tau$  model can be constrained by looking for the decay of the charged kaon associated with the  $L_\mu - L_\tau$  gauge boson. More concretely, we consider searches for single muon tracks from the decays of stopped charged kaons as performed in the E949 experiment. As a result, we find that favored parameter region for the muon anomalous magnetic moment can be tested by using 10 times larger number of stopped charged kaons and about 100 times better photon rejection rate than the E949 experiment.

---

\* e-mail: ibe@icrr.u-tokyo.ac.jp

† e-mail: m156077@icrr.u-tokyo.ac.jp

‡ e-mail: m0t@icrr.u-tokyo.ac.jp

## I. INTRODUCTION

The Standard Model (SM) of particle physics has passed high precision experimental tests for decades as the best description of electroweak and strong interactions. Despite this overwhelming success, however, there is a long-standing discrepancy between the SM prediction [1–3] and the experimental value [4–6] at more than  $3\sigma$  level,

$$\delta a_\mu = a_\mu^{\text{exp}} - a_\mu^{\text{SM}} = (287 \pm 80) \times 10^{-11} . \quad (1)$$

Future experiments, such as E34 [7] (an ultra-cold muon beam experiment) and E989 [8] (an improved version of E821), are expected to reduce experimental uncertainties by a factor of four which would confirm the discrepancy at the  $5\sigma$  level.

In order to resolve the discrepancy, so far, many SM extensions have been proposed [see 9, for review]. Among various proposals, a class of models with a new  $U(1)$  gauge symmetry provides one of the most minimal extensions. There, the muon anomalous magnetic moment receives a contribution from the new massive gauge boson  $Z'$  at the one-loop level which reduces the discrepancy.

The models with a new  $U(1)$  gauge symmetry are, however, severely constrained from various experimental searches. For example, when the new  $U(1)$  gauge symmetry is identified with the  $B - L$  gauge symmetry, the parameter region which resolves the discrepancy is excluded by neutrino-electron scattering experiments [10, 11]. Models with a dark photon are also studied extensively, where the dark photon has kinetic mixing with the SM photon. However, those models are also excluded as a solution to the discrepancy by electron beam dump experiments [12–17] and by  $e^+e^-$  collider experiments [18].<sup>1</sup>

To evade those constraints, many models with lepton non-universal gauge charges have been discussed [21–31]. In particular, the model with  $L_\mu - L_\tau$  gauge interaction [21, 22] is the least constrained one due to its lack of interactions to electrons, electron-type neutrinos, and quarks. Currently, the most stringent constraint on this model comes from the neutrino trident production experiments [32, 33]. The gauge boson mass,  $m_{Z'}$ , larger than about 400 MeV is excluded in the parameter region favored by the muon anomalous magnetic moment [34]. Some portion of the favored parameter region has been also excluded by

---

<sup>1</sup> Some of the constraints can be relaxed by assuming light dark matter into which the dark photon decays (see e.g. Refs. [19, 20]).

TABLE I. The charge assignment of the  $L_\mu - L_\tau$  gauge symmetry. Here, all the fermions are left-handed Weyl fermions. The SM fields not in the table are not charged under the  $L_\mu - L_\tau$ .

	$\ell_{\mu L} = (\nu_{\mu L}, \mu_L)^T$	$\ell_{\tau L} = (\nu_{\tau L}, \tau_L)^T$	$\bar{\mu}_R$	$\bar{\tau}_R$	$\bar{N}_{\mu R}$	$\bar{N}_{\tau R}$
$L_\mu - L_\tau$	1	-1	-1	1	-1	1

the searches for the  $\mu^+\mu^-$  pair production associated with  $Z'$  decaying into  $\mu^+\mu^-$  pair for  $m_{Z'} \gtrsim 2 \times m_\mu \simeq 211 \text{ MeV}$  [35] (see Fig. 1). Here,  $m_\mu$  is the muon mass.

For  $m_{Z'} \lesssim 2 \times m_\mu$ , on the other hand,  $Z'$  dominantly decays into neutrinos, which makes the experimental test of this model even harder. In this paper, we discuss how the  $L_\mu - L_\tau$  model can be constrained by looking for the decay of the charged kaon associated with  $Z'$ , i.e.  $K^+ \rightarrow \mu^+ + \nu_\mu + Z' (\rightarrow \nu\bar{\nu})$  where all the neutrinos in the final states are invisible. As we will see, the favored parameter region for the muon anomalous magnetic moment can be tested by using 10 times larger number of stopped charged kaons and about 100 times better photon rejection rate than the E949 experiment [36, 37].

The organization of the paper is as follows. In section II, we summarize the  $L_\mu - L_\tau$  model. In section III, we discuss the testability of the model by using the decay of the stopped charged kaon associated with  $Z'$ . Final section is devoted to our conclusions.

## II. $L_\mu - L_\tau$ MODEL

The lepton numbers for each flavor,  $L_i = (L_e, L_\mu, L_\tau)$ , are not free from the anomalies of the Standard Model gauge symmetry. The differences between the lepton numbers,  $L_i - L_j$  ( $i \neq j$ ), are, on the other hand, free from anomalies. Thus, they can be gauge symmetries without adding any extra charged fermions [21, 22]. Among them, the model with the  $L_\mu - L_\tau$  gauge symmetry does not have interactions to electrons, to electron-type neutrinos, and to quarks.

The gauge charge assignment of the  $L_\mu - L_\tau$  gauge symmetry is given in Table I. Assuming that the  $L_\mu - L_\tau$  gauge symmetry is broken spontaneously, the  $L_\mu - L_\tau$  gauge boson,  $Z'$ , couples to the SM fields through the Lagrangian,

$$\mathcal{L}_{Z'} = -\frac{1}{4}F_{Z'\mu\nu}F_{Z'}^{\mu\nu} + \frac{1}{2}m_{Z'}^2 Z'_\mu Z'^\mu - g_{Z'} Z'_\mu j_{Z'}^\mu, \quad (2)$$

$$j_{Z'}^\mu = \ell_{\mu L}^\dagger \bar{\sigma}^\mu \ell_{\mu L} - \ell_{\tau L}^\dagger \bar{\sigma}^{\tau L} \ell_{\tau L} - \bar{\mu}_R^\dagger \bar{\sigma}^\mu \bar{\mu}_R + \bar{\tau}_R^\dagger \bar{\sigma}^\mu \bar{\tau}_R - \bar{N}_{\mu R}^\dagger \bar{\sigma}^\mu \bar{N}_{\mu R} + \bar{N}_{\tau R}^\dagger \bar{\sigma}^\mu \bar{N}_{\tau R}, \quad (3)$$

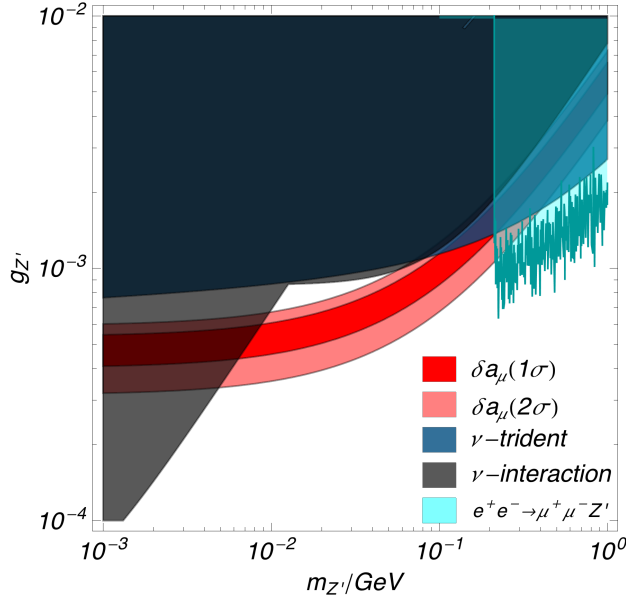


FIG. 1. Parameter region which explains the muon anomalous magnetic moment within  $1\sigma$  (red) and  $2\sigma$  (pink). The dark blue shaded region is excluded by the results of the neutrino trident production experiments [34]. The gray shaded region is excluded by the results of the neutrino-electron scattering experiments [10, 11]. The cyan shaded region is excluded by the searches for the  $\mu^+\mu^-$  pair production associated with  $Z'$  decaying into  $\mu^+\mu^-$  [35]. (Similar figure is given in [42].)

where  $F_{Z'}$ ,  $m_{Z'}$ , and  $g_{Z'}$  denote the field strength, the mass and the gauge coupling constant of  $Z'$ , respectively. In the current  $j_{Z'}^\mu$ ,  $\ell_{\mu,\tau L}$ ,  $\bar{\mu}_R$ , and  $\bar{\tau}_R$  denote the  $\mu$  and  $\tau$  doublet leptons,  $\mu$  and  $\tau$  singlet leptons, respectively. Here, we also include the right-handed neutrinos  $\bar{N}_R$  with which the neutrinos in the SM obtain masses via the see-saw mechanism [38, 39] [see also 40].<sup>2</sup> We assume that  $\bar{N}_R$ 's obtain masses of the order of the  $L_\mu - L_\tau$  breaking scale, i.e.  $\mathcal{O}(m_{Z'}/g_{Z'})$ , and hence, they do not play crucial roles for phenomenology in the following discussion.

### A. Muon anomalous magnetic moment

Due to the non-vanishing muon charges,  $Z'$  contributes to the muon anomalous magnetic moment which is given by,

$$\delta a_\mu = \frac{g_{Z'}^2}{8\pi^2} \int_0^1 dx \frac{2m_\mu^2 x^2 (1-x)}{x^2 m_\mu^2 + (1-x)m_{Z'}^2}, \quad (4)$$

<sup>2</sup> See e.g. [41] for a model which can reproduce the observed neutrino mixing angles.

at the one-loop level. In Fig. 1, we show the parameter region favored by the muon anomalous magnetic moment within  $1\sigma$  range as a red band. The figure shows that the discrepancy of the muon anomalous magnetic moment can be explained for  $g_{Z'} \sim 5 \times 10^{-4}$  for  $m_{Z'} \ll m_\mu$  and  $g_{Z'} \sim 5 \times 10^{-3}(m_{Z'}/1 \text{ GeV})$  for  $m_{Z'} \gg m_\mu$ .

## B. Neutrino Trident Production

The results of the searches for the neutrino trident production,  $\nu_\mu + N \rightarrow \nu_\mu + N + \mu^+ + \mu^-$ , put stringent constraints on the  $L_\mu - L_\tau$  model where  $N$  denotes a target nucleus [34]. In the SM, the neutrino trident production is mediated by the  $W$  and  $Z$  boson exchanges. Similarly, the  $L_\mu - L_\tau$  interactions also contribute to the neutrino trident production via the  $Z'$  exchange. The production cross section estimated from the CCFR experiment [33] is in good agreement with the SM prediction

$$\sigma_{CCFR}/\sigma_{SM} = 0.82 \pm 0.28 , \quad (5)$$

which leaves only a small room for the contribution from the  $L_\mu - L_\tau$  interactions.<sup>3</sup>

In Fig. 1, we show the 95% CL exclusion limit on the  $L_\mu - L_\tau$  model from the neutrino trident production. Here, we use the equivalent photon approximation to estimate the production cross section according to [34]. The figure shows that the region favored by the muon anomalous magnetic moment is excluded for  $m_{Z'} \gtrsim 400 \text{ MeV}$ .

## C. Neutrino-Electron Interactions

So far, we have assumed that the kinetic mixing between the photon and  $Z'$ ,

$$\mathcal{L}_{\text{mix}} = \frac{1}{2} \epsilon F_{\mu\nu} F_{Z'}^{\mu\nu} , \quad (6)$$

is vanishing. Such a kinetic mixing is, however, generated radiatively even if we assume that it is vanishing at the tree-level. At the one-loop level, the induced kinetic mixing is given

---

<sup>3</sup> The CHARM-II collaboration also reported the trident event rate which is consistent with the SM prediction [32], from which we obtain less stringent constraints on the  $L_\mu - L_\tau$  interactions.

by,

$$\epsilon = \frac{8}{3} \frac{eg_{Z'}}{16\pi^2} \log \frac{m_\tau}{m_\mu} , \quad (7)$$

where  $e$  is the QED coupling constant.<sup>4</sup>

Once  $Z'$  has kinetic mixing to the photon,  $Z'$  obtains couplings to the QED current  $j_{\text{QED}}^\mu$

$$\mathcal{L} = -\epsilon e Z'_\mu j_{\text{QED}}^\mu , \quad (8)$$

after eliminating the kinetic mixing term by shifting the photon fields. Thus, the  $L_\mu - L_\tau$  model can be further constrained via the interactions to the electrons and quarks.<sup>5</sup> In particular, the neutrino-electron scattering experiments put stringent constraints [10, 11].

In Fig. 1, we show the constraints from the neutrino-electron scattering experiments at the 90% CL exclusion limit. which are translated from the ones obtained in [11]. It should be noted that the  $L_\mu - L_\tau$  model cannot be constrained by the experiments using  $\nu_e$  nor  $\bar{\nu}_e$  unless they oscillate into other flavors. Thus, the TEXONO experiments [43–45] which put the most stringent constraints on the flavor universal gauge interactions do not constrain the  $L_\mu - L_\tau$  model. As a result, we find that the main constraints come from the CHARM-II experiment [46, 47] for  $m_{Z'} \gtrsim 200$  MeV which uses the  $\nu_\mu$  and  $\bar{\nu}_\mu$  beams, and from the BOREXINO experiment [48] for  $m_{Z'} \lesssim 200$  MeV where about a half of  ${}^7\text{Be}$  solar neutrinos oscillate into other neutrinos.

#### D. $e^+ + e^-$ Collider Experiment

The BaBar experiments put constraints on  $\mu^+\mu^-$  pair production associated with  $Z'$  decaying into  $\mu^+\mu^-$  [35]. In Fig. 1, we show the constraints on the parameter space at the 90% CL translated from [35].

Let us also comment on the beam dump experiments utilizing the electron or the proton beams which put stringent bounds on the sub-GeV dark photon models with kinetic mixing to the photon of  $\epsilon \sim 10^{-(5-6)}$  [49]. In the  $L_\mu - L_\tau$  model, although non-vanishing kinetic

<sup>4</sup> At the level of the QED, the kinetic mixing is forbidden by a discrete symmetry,  $\mu \leftrightarrow \tau$ ,  $F^{\mu\nu} \rightarrow F^{\mu\nu}$ , and  $F_{Z'}^{\mu\nu} \rightarrow -F_{Z'}^{\mu\nu}$  in the limit of  $m_\mu = m_\tau$ . By the soft symmetry breaking  $m_\mu \neq m_\tau$ , radiative corrections generate finite kinetic mixing.

<sup>5</sup> The interactions to electron-type neutrinos are still suppressed since the effects of kinetic mixing to  $Z$  boson are suppressed by  $m_{Z'}^2/m_Z^2$ .

mixing in Eq. (7) of  $10^{-(5-6)}$  is expected,  $Z'$  in the  $L_\mu - L_\tau$  model immediately decays into neutrinos, and hence, they do not lead to stringent limits.

### E. Other Constraints

Before closing this section, let us discuss other constraints which are not shown in Fig. 1. First, in order not to spoil the success of the Big-Bang Nucleosynthesis (BBN), the extra contributions to the effective number of relativistic species at around the BBN temperature,  $N_{\text{eff}}$ , are constrained to be  $\Delta N_{\text{eff}} \lesssim 1$  [50, 51]. This constraint puts lower limit on the  $Z'$  mass,  $m_{Z'} \gtrsim 5 \text{ MeV}$  [52].

When  $Z'$  mass is around or below the typical core temperature of the supernovae,  $T \sim 30 \text{ MeV}$ ,  $Z'$  can be produced inside the cores of the supernovae. The presence of  $Z'$  in the supernova cores can affect the diffusion times of neutrinos which should be around 10 s estimated from the observed duration of the neutrino burst of SN1987A [53, 54]. According to Ref. [52], the parameter region favored by the muon anomalous magnetic moment can be excluded for  $m_{Z'} \lesssim 30\text{--}50 \text{ MeV}$ .

For  $m_{Z'} > 2m_\mu$ , the SM  $Z$  boson decays into a pair of  $\mu^+\mu^-$  associated with the  $Z'$  production which subsequently decays into  $\mu^+\mu^-$  [28, 41, 55]. However, the resultant constraints from the LHC experiments are less stringent from the ones shown in Fig. 1.

In summary, the  $L_\mu - L_\tau$  interactions can successfully resolve the discrepancy of the muon anomalous magnetic moment for  $\mathcal{O}(1) \text{ MeV} \lesssim m_{Z'} \lesssim 400 \text{ MeV}$  and  $g_{Z'} \sim 10^{-3}$ , while evading all the experimental constraints. In the following, we discuss how we can test the remaining parameter region by using the rare kaon decay.

### III. RARE KAON DECAY

For  $m_{Z'} < 2 \times m_\mu$ ,  $Z'$  boson which associates with the charged kaon decay,  $K^+ \rightarrow \mu^+ + \nu_\mu + Z'$ , results in  $K^+ \rightarrow \mu^+ + \text{invisible}$ . This mode can be distinguished from the main mode of the charged kaon,  $K^+ \rightarrow \mu^+ + \nu_\mu$ , in which the muon momentum is  $p_\mu = 236 \text{ MeV}$  while the muon in the  $K^+ \rightarrow \mu^+ + \nu_\mu + Z'$  mode possesses a continuous spectrum.<sup>6</sup> (See

---

<sup>6</sup> The branching ratio of the irreducible background in the SM,  $K^+ \rightarrow \mu^+ + \nu_\mu + \nu + \bar{\nu}$ , is  $\mathcal{O}(10^{-16})$  [56].

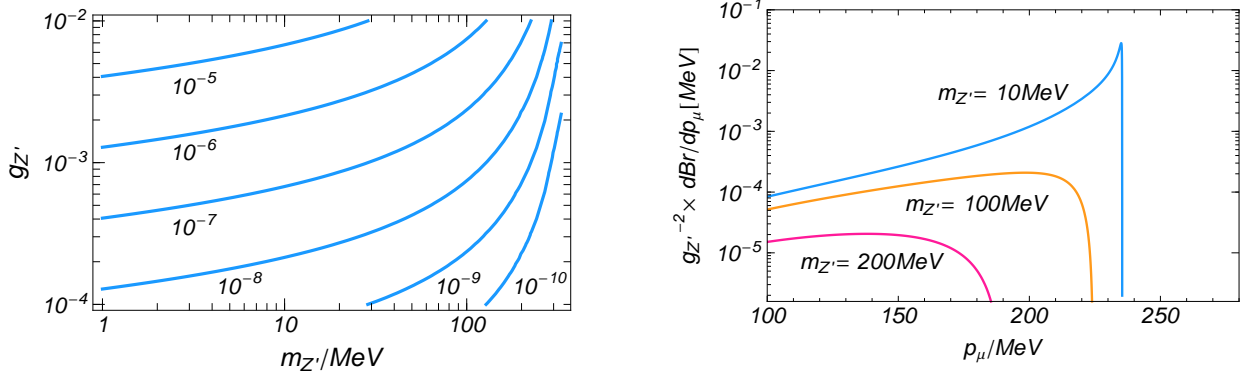


FIG. 2. Left) The branching ratio of  $K^+$  into  $K^+ \rightarrow \mu^+ + \nu_\mu + Z'$ . Right) The differential branching ratio normalized by  $g_{Z'}^{-2}$  for given  $Z'$  masses.

[57–59] for earlier works to utilize  $K^+ \rightarrow \mu + \text{invisible}$  mode to put constraints on light particles coupling to the muon.)

The amplitude for  $K^+ \rightarrow \mu^+ + \nu_\mu + Z'$  is given by

$$\mathcal{M} = -i2f_K V_{us} G_F \times \varepsilon^{\nu*}(Z') \left\{ \bar{u}(\nu_\mu) P_R \not{\ell} \frac{2p_\nu + \not{\ell} \gamma_\nu}{2p \cdot q + q^2} v(\mu^+) - \bar{u}(\nu_\mu) P_R \frac{(2k_\nu + \gamma_\nu \not{\ell})}{2k \cdot q + q^2} \not{\ell} v(\mu^+) \right\}, \quad (9)$$

where  $G_F$  is the Fermi constant,  $V_{us} \simeq 0.23$  the CKM angle, and  $f_K$  the kaon decay constant. The four momenta of  $\mu^+$ ,  $\nu_\mu$ ,  $Z'$  and  $K^+$  are given by  $p$ ,  $k$ ,  $q$  and  $\ell$ . The wave functions of  $\mu^+$ ,  $\nu_\mu$  and  $Z'$  are given by  $v(\mu^+)$ ,  $u(\nu_\mu)$ , and  $\varepsilon(Z')$ , respectively.

In Fig. 2, we show the branching ratio and the muon momentum spectrum in the  $L_\mu - L_\tau$  model. So far, the upper limit on the branching ratio into  $K^+ \rightarrow \mu^+ + \text{invisible}$  is  $6 \times 10^{-6}$  at the 90% CL which has been put by looking for the muon tracks in the momentum range 128 MeV to 176 MeV from the decays of the stopped charged kaons at the LBL Bevatron [60]. Compared with the predicted branching ratio in Fig. 2, we find that this bound does not exclude the parameter region favored by the muon anomalous magnetic moment.

To put more stringent constraint, we consider the results of the search for heavy neutrinos in the decay of the stopped charged kaon by E949 experiment [37]. There, they looked for the muon tracks in the momentum range 140 MeV to 200 MeV with an total exposure of  $N_K^{\text{E949}} = 1.70 \times 10^{12}$  stopped kaons.<sup>7</sup> The main background to the signal comes from the radiative decay mode,  $K^+ \rightarrow \mu^+ + \nu_\mu + \gamma$ , with a missing photon.<sup>8</sup> In the E949 experiment,

<sup>7</sup> Typically,  $1.6 \times 10^6$  kaons per second enter the stopping target.

<sup>8</sup> The decay modes involving charged pions are effectively vetoed by the Range-Momentum cut [37].



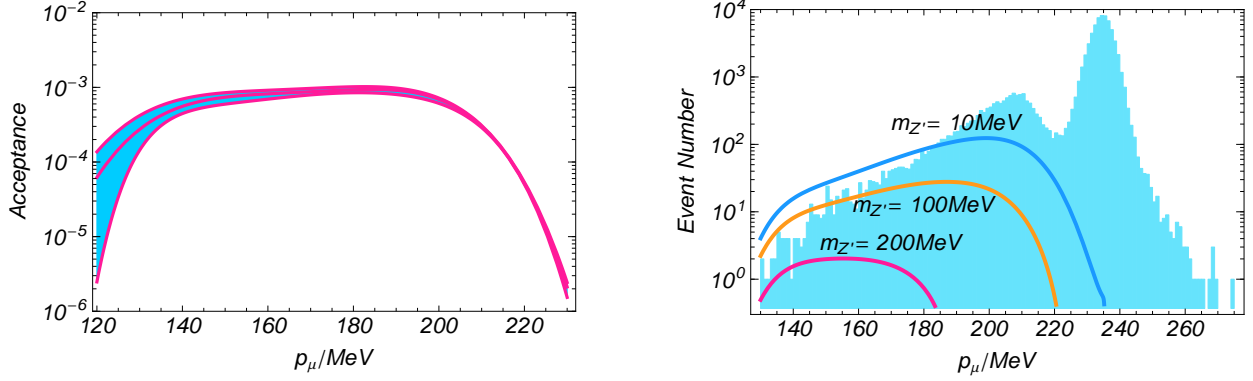


FIG. 3. Left) The single muon acceptance in E949 experiment after all the cuts are applied given in [37]. The band corresponds to  $1\sigma$  error of the acceptance. Right) The signal spectrum expected at the E949 experiment where the muon acceptance is assumed to be the lower one in the left panel. We also show the observed event numbers at the E949 experiment after tight photon veto cuts.

a typical photon rejection rate is around  $\epsilon_\gamma^{\text{E949}} \sim 10^{-3}$  after tight photon veto cuts. By comparing with the branching ratio [6],<sup>9</sup>

$$BR(K^+ \rightarrow \mu^+ + \nu_\mu + \gamma, 140 \text{ MeV} < p_\mu < 200 \text{ MeV}) = (1.4 \pm 0.2) \times 10^{-3}, \quad (10)$$

we expect that the results of the E949 experiment can put the limits on the branching ratio into  $Z'$  of  $\mathcal{O}(10^{-6})$ . In fact, the E949 collaboration recently reported a constraint on  $BR(K^+ \rightarrow \mu + \nu\nu\bar{\nu}) \lesssim 2.4 \times 10^{-6}$  at the 90% CL [61] by assuming non-standard dimension six neutrino interactions [62].

In the left panel of Fig.3, we show the single muon acceptance after all the cuts are applied [37]. The figure shows that the acceptance is around  $10^{-3}$  for  $140 \text{ MeV} < p_\mu < 200 \text{ MeV}$ . The band corresponds to the  $1\sigma$  error of the muon acceptance for a given muon momentum. In the right panel, we also show the expected muon spectrum in the  $L_\mu - L_\tau$  model at E949 experiment for  $g_{Z'} = 10^{-2}$ . Here, we assume the lower muon acceptance in the left panel to make our analysis conservative. The histogram in the figure shows the observed event numbers at E949 after tight photon veto cuts.

In order to estimate exclusion limit on the gauge coupling constant for a given  $m_{Z'}$ , we combine the event numbers in the momentum bins from  $p_\mu = 130 \text{ MeV}$  to  $p_\mu = 160 \text{ MeV}$

<sup>9</sup> In this momentum range, the so-called internal bremsstrahlung dominates the radiative decay.

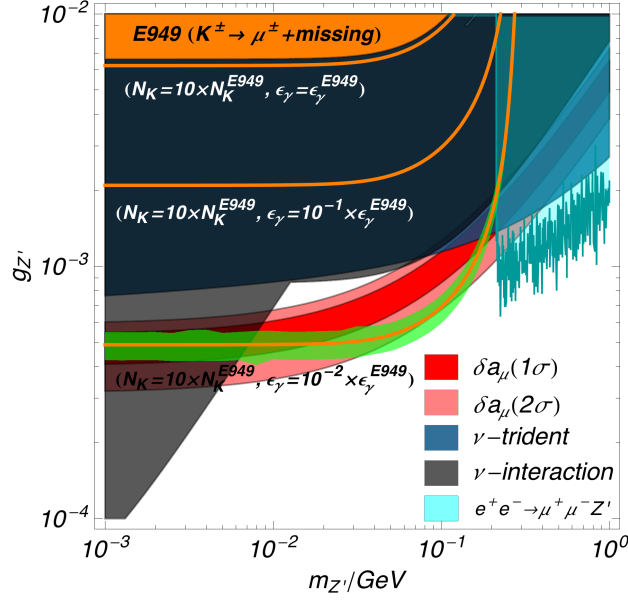


FIG. 4. The 95 % CL limit from the E949 experiment (orange shaded region) overlaid on Fig. 1. We also show the possible improved sensitivities by assuming several setups as indicated in the figure. The green band around the expected exclusion limit for  $N_K = 10 \times N_K^{E949}$  and  $\epsilon_\gamma = 10^{-2} \times \epsilon_\gamma^{E949}$  corresponds to the  $2\sigma$  statistical fluctuation of the expected exclusion limit.

and use a test statistic,

$$-2 \ln \lambda = 2 \left( N_s - N_{\text{obs}} + N_{\text{obs}} \ln \frac{N_{\text{obs}}}{N_s} \right), \quad (11)$$

where  $N_{\text{obs}}$  and  $N_s$  are the total observed and the total expected signal event numbers in the momentum bins from  $p_\mu = 130$  MeV to  $p_\mu = 160$  MeV. It should be noted that more stringent limit can be obtained if we can predict the number of the background events including the detector responses accurately, which goes beyond the scope of our paper.

In Fig. 4, we show the 95 % CL limit from the E949 experiment as orange shaded region. Here, we define the 95 % CL limit by  $-2 \ln \lambda > \chi_{95}^2 = 3.842$  assuming that  $N_s \gg 1$ . The figure shows that the results of the E949 experiment exclude the parameter region corresponding to the branching ratio into  $Z'$  of  $\mathcal{O}(10^{-6})$  as expected. It should be noted that the exclusion limit is insensitive to  $m_{Z'}$  in a lighter  $Z'$  region while the predicted branching in Fig. 2 is larger for a lighter  $Z'$  for a given  $g_{Z'}$ . This behavior can be understood from the spectrum shapes of the signal in Fig. 3 where it becomes closer to the one of the background for a lighter  $Z'$  and hence  $N_s$  becomes less sensitive to  $m_{Z'}$  in that region.

Now, let us discuss how the constraint can be improved by assuming several experimental setups. First, let us assume 10 times larger exposure,  $N_K = 10 \times N_K^{E949}$ , while assuming the same muon acceptance and the same photon rejection rate with the E949 experiment. In E949 experiment,  $5 \times 10^5$  kaons are yielded from every  $10^{12}$  p.o.t. [36]. Thus, such a high intensity is possible if we assume the proton beam of  $\mathcal{O}(10^{20})$  p.o.t. which corresponds to the assumption for the SHIP experiment [63]. As the figure shows, however, the expected exclusion limit is not very much improved.

Next, let us assume 10 and 100 times better photon rejection rates compare with the E949 experiments while assuming the same muon acceptance. For feasibility of those high rejection rates, see e.g. [64]. The figure shows that with the 100 times better photon rejection rates with  $N_K = 10 \times N_K^{E949}$ , the large portion of the parameter region favored by the muon anomalous magnetic moment can be tested.<sup>10</sup> In the figure, we also show the  $2\sigma$  statistical fluctuation of the expected exclusion limit for the case with 100 times better photon rejection rate (see the appendix A).

Before closing this section, let us comment on constraints from kaon experiments in which the kaons decay in-flight as in the NA62 experiment [65] and the SHIP experiment [63]. In those types of experiments, the muons in the beams contaminate the kaon beams in the decay region. Those muon beams contribute to background events for the searches of a single muon in  $K^+ \rightarrow \mu + \text{invisible}$ . Thus, in the in-flight kaon decay experiments, it is important to develop a veto system to reject muons in beams while accepting the muons from the decay of the kaons.

#### IV. CONCLUSIONS

The model with the  $L_\mu - L_\tau$  gauge symmetry is the least constrained model as a resolution to the discrepancy of the muon anomalous magnetic moment between the theoretical prediction and the experimental result. There, the gauge boson of the  $L_\mu - L_\tau$  gauge symmetry,  $Z'$ , has highly suppressed interactions to electrons, to electron-type neutrinos, and to quarks. The experimental test of the model is particularly difficult when the  $Z'$  mass is lower than the muon pair threshold.

---

<sup>10</sup> For the 100 times better, the observed number to be excluded  $N_{\text{obs}} = 3$  in the momentum bin we are using, which corresponds to  $N_s \simeq 8$ . Thus, the 95% CL can be fairly approximated by  $-2 \ln \lambda > \chi_{95}^2$ .

In this paper, we discussed how well the  $L_\mu - L_\tau$  model can be tested as a resolution of the discrepancy of the muon anomalous magnetic moment by looking for the decay of the charged kaon associated with  $Z'$ . In our analysis, we consider the constraints by looking for a single muon track from the decay of the stopped charged kaons as performed in the E949 experiment [37, 61]. As a result, we find that the large portion of the favored parameter region for the muon anomalous magnetic moment can be tested by using 10 times larger number of stopped charged kaons and about 100 times better photon rejection rate.

## ACKNOWLEDGMENTS

MI thank Satoshi Shirai for useful discussion. This work is supported in part by Grants-in-Aid for Scientific Research from the Ministry of Education, Culture, Sports, Science, and Technology (MEXT), Japan, No. 25105011 and No. 15H05889 (M. I.); Grant-in-Aid No. 26287039 (M. I.) from the Japan Society for the Promotion of Science (JSPS); and by the World Premier International Research Center Initiative (WPI), MEXT, Japan.

## Appendix A: Statistical Fluctuation of the Expected Exclusion Limits

In order to estimate the statistical fluctuation of the expected exclusion limit, we generate mock data samples based on a background model. For that purpose, we use the fitted spectrum shown in Fig. 5 as a background model since it is difficult to have precise background model including the detector responses. To generate the mock data for various assumptions, we simply scale the fitted spectrum by factors of  $N_K/N_K^{\text{E949}}$  and  $\epsilon_\gamma/\epsilon_\gamma^{\text{E949}}$ .

In the right panel of Fig. 5, we show the statistical fluctuations of the expected exclusion limits at the 95% CL for various assumptions. Here, we use the same statistical analysis used in the main text (see discussion around Eq. (11)). For the original setup of the E949 experiment, the mean expected limit is slightly more stringent than the observed one in Fig. 4. This discrepancy indicates that our fitted spectrum slightly deviates from the true background model, although the discrepancy is within  $2\sigma$  range. As for the statistical fluctuations around the mean expected limit, on the other hand, they are not very sensitive to the shape of the background spectrum. In Fig. 4 in the main text, we show the fluctuation for  $N_K = 10 \times N_K^{\text{E949}}$  and  $\epsilon_\gamma = 10^{-2} \times \epsilon_\gamma^{\text{E949}}$  in Fig. 5 around the expected exclusion limit in

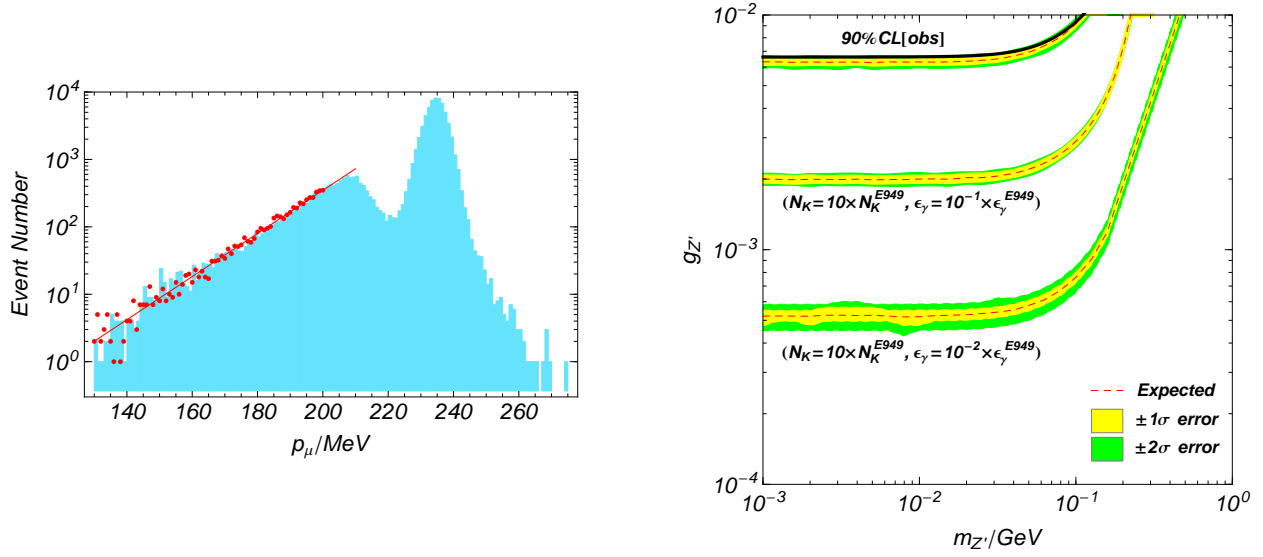


FIG. 5. Left) The fitted spectrum used to generate mock sample data sets (red line). One example of the mock data is also shown as red points. Right) The statistical fluctuations of the expected exclusion limits at 95% CL for various assumptions. The yellow shaded bands and the green bands correspond to  $1\sigma$  and  $2\sigma$  statistical fluctuations, respectively. The dashed line show the mean expected exclusion limit. The black line is the observed exclusion limit obtained in the main text by using the E949 data.

the analysis of the main text.

- 
- [1] M. Davier, A. Hoecker, B. Malaescu, and Z. Zhang, Eur. Phys. J. **C71**, 1515 (2011), [Erratum: Eur. Phys. J. **C72**, 1874 (2012)], arXiv:1010.4180 [hep-ph].
  - [2] F. Jegerlehner and R. Szafron, Eur. Phys. J. **C71**, 1632 (2011), arXiv:1101.2872 [hep-ph].
  - [3] G.-C. Cho, K. Hagiwara, Y. Matsumoto, and D. Nomura, JHEP **11**, 068 (2011), arXiv:1104.1769 [hep-ph].
  - [4] G. W. Bennett *et al.* (Muon g-2), Phys. Rev. **D73**, 072003 (2006), arXiv:hep-ex/0602035 [hep-ex].
  - [5] P. J. Mohr, B. N. Taylor, and D. B. Newell, Rev. Mod. Phys. **84**, 1527 (2012), arXiv:1203.5425 [physics.atom-ph].
  - [6] K. A. Olive *et al.* (Particle Data Group), Chin. Phys. **C38**, 090001 (2014).
  - [7] M. Aoki *et al.*, <http://g-2.kek.jp/portal/documents.html>.
  - [8] J. Grange *et al.* (Muon g-2), (2015), arXiv:1501.06858 [physics.ins-det].
  - [9] F. Jegerlehner and A. Nyffeler, Phys. Rept. **477**, 1 (2009), arXiv:0902.3360 [hep-ph].

- [10] R. Harnik, J. Kopp, and P. A. N. Machado, JCAP **1207**, 026 (2012), arXiv:1202.6073 [hep-ph].
- [11] S. Bilmis, I. Turan, T. M. Aliev, M. Deniz, L. Singh, and H. T. Wong, Phys. Rev. **D92**, 033009 (2015), arXiv:1502.07763 [hep-ph].
- [12] S. Andreas, C. Niebuhr, and A. Ringwald, Phys. Rev. **D86**, 095019 (2012), arXiv:1209.6083 [hep-ph].
- [13] D. Babusci *et al.* (KLOE-2), Phys. Lett. **B720**, 111 (2013), arXiv:1210.3927 [hep-ex].
- [14] P. Adlarson *et al.* (WASA-at-COSY), Phys. Lett. **B726**, 187 (2013), arXiv:1304.0671 [hep-ex].
- [15] G. Agakishiev *et al.* (HADES), Phys. Lett. **B731**, 265 (2014), arXiv:1311.0216 [hep-ex].
- [16] H. Merkel *et al.*, Phys. Rev. Lett. **112**, 221802 (2014), arXiv:1404.5502 [hep-ex].
- [17] J. R. Batley *et al.* (NA48/2), Phys. Lett. **B746**, 178 (2015), arXiv:1504.00607 [hep-ex].
- [18] J. P. Lees *et al.* (BaBar), Phys. Rev. Lett. **113**, 201801 (2014), arXiv:1406.2980 [hep-ex].
- [19] H. Davoudiasl, H.-S. Lee, and W. J. Marciano, Phys. Rev. **D89**, 095006 (2014), arXiv:1402.3620 [hep-ph].
- [20] K. Harigaya and Y. Nomura, Phys. Rev. **D94**, 035013 (2016), arXiv:1603.03430 [hep-ph].
- [21] R. Foot, Mod. Phys. Lett. **A6**, 527 (1991); R. Foot, X. G. He, H. Lew, and R. R. Volkas, Phys. Rev. **D50**, 4571 (1994), arXiv:hep-ph/9401250 [hep-ph].
- [22] X.-G. He, G. C. Joshi, H. Lew, and R. R. Volkas, Phys. Rev. **D44**, 2118 (1991).
- [23] S. N. Gninenko and N. V. Krasnikov, Phys. Lett. **B513**, 119 (2001), arXiv:hep-ph/0102222 [hep-ph].
- [24] S. Baek, N. G. Deshpande, X. G. He, and P. Ko, Phys. Rev. **D64**, 055006 (2001), arXiv:hep-ph/0104141 [hep-ph].
- [25] B. Murakami, Phys. Rev. **D65**, 055003 (2002), arXiv:hep-ph/0110095 [hep-ph].
- [26] E. Ma, D. P. Roy, and S. Roy, Phys. Lett. **B525**, 101 (2002), arXiv:hep-ph/0110146 [hep-ph].
- [27] M. Pospelov, Phys. Rev. **D80**, 095002 (2009), arXiv:0811.1030 [hep-ph].
- [28] J. Heeck and W. Rodejohann, Phys. Rev. **D84**, 075007 (2011), arXiv:1107.5238 [hep-ph].
- [29] C. D. Carone, Phys. Lett. **B721**, 118 (2013), arXiv:1301.2027 [hep-ph].
- [30] J. Heeck, Phys. Lett. **B758**, 101 (2016), arXiv:1602.03810 [hep-ph].
- [31] W. Altmannshofer, C.-Y. Chen, P. S. B. Dev, and A. Soni, Phys. Lett. **B762**, 389 (2016), arXiv:1607.06832 [hep-ph].
- [32] D. Geiregat *et al.* (CHARM-II), Phys. Lett. **B245**, 271 (1990).

- [33] S. R. Mishra *et al.* (CCFR), Phys. Rev. Lett. **66**, 3117 (1991).
- [34] W. Altmannshofer, S. Gori, M. Pospelov, and I. Yavin, Phys. Rev. Lett. **113**, 091801 (2014), arXiv:1406.2332 [hep-ph].
- [35] J. P. Lees *et al.* (BaBar), Phys. Rev. **D94**, 011102 (2016), arXiv:1606.03501 [hep-ex].
- [36] A. V. Artamonov *et al.* (BNL-E949), Phys. Rev. **D79**, 092004 (2009), arXiv:0903.0030 [hep-ex].
- [37] A. V. Artamonov *et al.* (E949), Phys. Rev. **D91**, 052001 (2015), [Erratum: Phys. Rev.D91,no.5,059903(2015)], arXiv:1411.3963 [hep-ex].
- [38] T. Yanagida, *Proceedings: Workshop on the Unified Theories and the Baryon Number in the Universe: Tsukuba, Japan, February 13-14, 1979*, Conf. Proc. **C7902131**, 95 (1979).
- [39] P. Ramond, in *International Symposium on Fundamentals of Quantum Theory and Quantum Field Theory Palm Coast, Florida, February 25-March 2, 1979* (1979) pp. 265–280, arXiv:hep-ph/9809459 [hep-ph].
- [40] P. Minkowski, Phys. Lett. **B67**, 421 (1977).
- [41] K. Harigaya, T. Igari, M. M. Nojiri, M. Takeuchi, and K. Tobe, JHEP **03**, 105 (2014), arXiv:1311.0870 [hep-ph].
- [42] T. Araki, F. Kaneko, T. Ota, J. Sato, and T. Shimomura, Phys. Rev. **D93**, 013014 (2016), arXiv:1508.07471 [hep-ph].
- [43] M. Deniz *et al.* (TEXONO), Phys. Rev. **D81**, 072001 (2010), arXiv:0911.1597 [hep-ex].
- [44] H. B. Li *et al.* (TEXONO), Phys. Rev. Lett. **90**, 131802 (2003), arXiv:hep-ex/0212003 [hep-ex]; H. T. Wong *et al.* (TEXONO), Phys. Rev. **D75**, 012001 (2007), arXiv:hep-ex/0605006 [hep-ex].
- [45] J.-W. Chen, H.-C. Chi, H.-B. Li, C. P. Liu, L. Singh, H. T. Wong, C.-L. Wu, and C.-P. Wu, Phys. Rev. **D90**, 011301 (2014), arXiv:1405.7168 [hep-ph].
- [46] P. Vilain *et al.* (CHARM-II), Phys. Lett. **B302**, 351 (1993).
- [47] P. Vilain *et al.* (CHARM-II), Phys. Lett. **B335**, 246 (1994).
- [48] G. Bellini *et al.*, Phys. Rev. Lett. **107**, 141302 (2011), arXiv:1104.1816 [hep-ex].
- [49] R. Essig, R. Harnik, J. Kaplan, and N. Toro, Phys. Rev. **D82**, 113008 (2010), arXiv:1008.0636 [hep-ph].
- [50] G. Mangano and P. D. Serpico, Phys. Lett. **B701**, 296 (2011), arXiv:1103.1261 [astro-ph.CO].
- [51] G. Steigman, Adv. High Energy Phys. **2012**, 268321 (2012), arXiv:1208.0032 [hep-ph].

- [52] A. Kamada and H.-B. Yu, Phys. Rev. **D92**, 113004 (2015), arXiv:1504.00711 [hep-ph].
- [53] K. Hirata *et al.* (Kamiokande-II), *GRAND UNIFICATION. PROCEEDINGS, 8TH WORKSHOP, SYRACUSE, USA, APRIL 16-18, 1987*, Phys. Rev. Lett. **58**, 1490 (1987), [,727(1987)].
- [54] R. M. Bionta *et al.*, Phys. Rev. Lett. **58**, 1494 (1987).
- [55] F. Elahi and A. Martin, Phys. Rev. **D93**, 015022 (2016), arXiv:1511.04107 [hep-ph].
- [56] D. Gorbunov and A. Mitrofanov, JHEP **10**, 039 (2016), arXiv:1605.08077 [hep-ph].
- [57] C. E. Carlson and B. C. Rislow, Phys. Rev. **D86**, 035013 (2012), arXiv:1206.3587 [hep-ph].
- [58] T. Beranek and M. Vanderhaeghen, Phys. Rev. **D87**, 015024 (2013), arXiv:1209.4561 [hep-ph].
- [59] R. Laha, B. Dasgupta, and J. F. Beacom, Phys. Rev. **D89**, 093025 (2014), arXiv:1304.3460 [hep-ph].
- [60] C. Y. Pang, R. H. Hildebrand, G. D. Cable, and R. Stiening, Phys. Rev. **D8**, 1989 (1973).
- [61] A. V. Artamonov *et al.* (E949), Phys. Rev. **D94**, 032012 (2016), arXiv:1606.09054 [hep-ex].
- [62] D. Yu. Bardin, S. M. Bilenky, and B. Pontecorvo, Phys. Lett. **B32**, 121 (1970).
- [63] M. Anelli *et al.* (SHiP), (2015), arXiv:1504.04956 [physics.ins-det].
- [64] E. Ramberg, P. Cooper, and R. Tschirhart, *Real-time. Proceedings, 13th Conference on Computing Applications in Nuclear and Plasma Sciences, RT2003, Montreal, Canada, May 18-23, 2003*, IEEE Trans. Nucl. Sci. **51**, 2201 (2004).
- [65] E. Goudzovski (NA48/2, NA62), (2012), arXiv:1208.2885 [hep-ex].